


Hyperfine anomaly in heavy atoms and its role in precision atomic searches for new physicsB. M. Roberts^{✉*} and J. S. M. Ginges^{✉†}*School of Mathematics and Physics, The University of Queensland, Brisbane QLD 4072, Australia* (Received 25 January 2021; revised 2 July 2021; accepted 10 August 2021; published 27 August 2021)

We report on our calculations of differential hyperfine anomalies in the nuclear single-particle model for a number of atoms and ions of interest for precision atomic tests of the standard model. It is shown that a comparison with available experimental data allows one to discriminate between different nuclear magnetization models. The nuclear single-particle model leads to significantly better agreement with experiment than the routinely used uniform ball model, and we advocate its use in future studies of the hyperfine structure. These results have implications for the uncertainty analyses of atomic structure theory that forms a critical part of the interpretation of precision atomic measurements, including the atomic parity violation measurement in cesium.

DOI: [10.1103/PhysRevA.104.022823](https://doi.org/10.1103/PhysRevA.104.022823)**I. INTRODUCTION**

Investigations of atomic parity violation provide some of the most constraining low-energy tests of electroweak theory [1–4]. These investigations require exquisitely precise measurements of parity-violating transition amplitudes [5–7], and equally precise atomic structure calculations [8–12] for their interpretation. Similarly, measurements of time-reversal-violating electric dipole moments (EDMs) in atoms and molecules require atomic and molecular structure theory for their interpretation in terms of fundamental charge-parity (CP)-violating parameters [13–16]. While such EDMs have eluded detection to date, the experimental programs are ramping up and their measurements clamping down on the size of these EDMs [17–25]. The implications for new CP -violating models are profound, demanding increasingly accurate theory for meaningful constraints and in anticipation of nonzero measurements.

The magnetic hyperfine structure, which arises due to the interaction of atomic electrons with the nuclear magnetic moment, plays an important role in precision studies of violations of fundamental symmetries. The testing and further development of atomic theory depends on comparisons between calculated and measured quantities that probe the atomic wave functions across all length scales of the atom. The quantities used for benchmarking include binding energies, electric dipole matrix elements, and hyperfine structure constants. It is the latter that allows unique access to the quality of the wave functions in the nuclear region, where the parity-violating and EDM interactions take place [1].

Hyperfine structure calculations depend on the modeling of nuclear structure effects. In particular, they are sensitive to the distribution of the nuclear magnetic moment across the nucleus, the so-called Bohr-Weisskopf (BW) effect [26,27]. It has been recognized only recently [28–30] that for a number

of heavy atoms of interest this dependence is much stronger than has been assumed. The effect is so large that in some cases the hyperfine splitting shifts by more than the claimed atomic theory uncertainty when switching from one nuclear magnetization model to another. Indeed, for Cs and Fr—of particular interest in atomic parity violation studies, and where the claimed atomic structure uncertainty has reached 0.5% or better—the hyperfine splittings change by as much as 0.5% and 1.5% when a simple nuclear single-particle model is used in place of the widely adopted uniform distribution. The ability to test the validity of these models is therefore of critical importance.

The most precise atomic parity violation measurement has been performed for Cs [5], and there are experiments underway in Cs [7] and Fr [31,32] and interest in studying Ba^+ , Ra^+ , and Rb [33–42]. Measurements of atomic parity violation across a chain of Yb isotopes have recently been performed [43], and while the considered ratios of measured values do not rely on the atomic structure for their interpretation, they strongly depend on the neutron distribution. Systems under recent and ongoing experimental investigation for detection of EDMs include the paramagnetic atoms Tl [17], Fr [44], and molecules YbF [18], BaF [22], and the diamagnetic systems Hg [20], Ra [19], and TlF [25].

In this paper, we calculate the BW effect and hyperfine anomalies for systems of interest for precision studies that may be treated as single-valence-electron atoms or ions and for which there is experimental data to compare—Rb, Cs, Ba^+ , Yb^+ , Hg^+ , and Tl. We recently studied these effects in Fr isotopes, leading to improved values for their nuclear moments [30]; they were studied more recently in Tl isotopes [45]. The differential hyperfine anomaly—the difference in the hyperfine structure for different isotopes of the same atom—arises due to finite nuclear size effects. We show that available experimental data allow one to distinguish between different nuclear magnetization models. These data support the use of the nuclear single-particle model [46–51], rather than the uniformly magnetized ball, for modeling the BW effect. This is bolstered by experimental

*b.roberts@uq.edu.au

†j.ginges@uq.edu.au

data for the hyperfine structure in H-like ions and muonic atoms.

There are other areas also where the BW effect plays a particularly important role. This includes in the determination of nuclear magnetic moments [30,52,53], and as a means of probing the neutron distribution [54,55]. Its problematic contribution to the hyperfine structure in tests of quantum electrodynamics in highly charged ions is removed in a carefully constructed difference of the effects in H-like and Li-like ions [56,57].

II. BOHR-WEISSKOPF EFFECT

The relativistic operator for the electron interaction with the nuclear magnetic moment is

$$h_{\text{hfs}} = \alpha \boldsymbol{\mu} \cdot (\mathbf{r} \times \boldsymbol{\alpha}) F(r)/r^3, \quad (1)$$

where $\boldsymbol{\alpha}$ is a Dirac matrix, $\boldsymbol{\mu} = \mu \mathbf{I}/I$ is the nuclear magnetic moment, \mathbf{I} is the nuclear spin, $F(r)$ describes the nuclear magnetization distribution [$F(r) = 1$ for a pointlike nucleus], and $\alpha \approx 1/137$ is the fine-structure constant (we use atomic units $\hbar = |e| = m_e = 1$, $c = 1/\alpha$). The expectation value of the operator (1) may be expressed as $\mathcal{A}(\mathbf{I} \cdot \mathbf{J})$, where \mathbf{J} is the electron angular momentum, and \mathcal{A} is the magnetic hyperfine constant.

The BW effect arises from the nuclear magnetization distribution and gives a significant contribution to the hyperfine structure [26]. For heavy atoms, it is standard to model the nucleus as a uniformly magnetized ball:

$$F_{\text{Ball}}(r) = \begin{cases} (r/r_m)^3, & r < r_m, \\ 1, & r \geq r_m, \end{cases} \quad (2)$$

with the nuclear magnetic radius typically taken as $r_m = \sqrt{5/3} r_{\text{rms}}$, where r_{rms} is the root-mean-square (rms) charge radius.

A more sophisticated modeling of the magnetization distribution taking into account the nuclear configuration may be given by the simple nuclear single-particle (SP) model [46–51]. For odd isotopes, we take the distribution presented in Ref. [50],

$$F_I(r) = F_{\text{Ball}}(r)[1 - \delta F_I \ln(r/r_m)\Theta(r_m - r)], \quad (3)$$

where Θ is the Heaviside step function and

$$\delta F_I = \begin{cases} \frac{3(2I-1)}{8(I+1)} \frac{4(I+1)g_L - g_S}{g_I I}, & I = L + 1/2, \\ \frac{3(2I+3)}{8(I+1)} \frac{4I g_L + g_S}{g_I I}, & I = L - 1/2. \end{cases} \quad (4)$$

Here, I , L , and S are the total, orbital, and spin angular momenta for the unpaired nucleon, $g_L = 1$ (0) for a proton (neutron), and $g_I = \mu/(\mu_N I)$ is the nuclear g -factor with μ_N the nuclear magneton. The spin g -factor g_S is chosen so that the experimental value for g_I is reproduced using the Landé g -factor expression. Formulas (3) and (4) are found by taking the radial part of the probability density of the nucleon to be constant across the nucleus. The model may be improved, e.g., by finding the nucleon wave function in a Woods-Saxon potential and including the spin-orbit interaction [49]. The effect of accounting for these has been shown to be small

($\lesssim 10\%$) for the BW effect in ^{87}Rb , ^{133}Cs , and ^{211}Fr [28], as well as in isotopes of Tl [45], and larger in $^{135}\text{Ba}^+$ and $^{225}\text{Ra}^+$ [28]. The single-particle model may be extended in a simple way to describe the magnetization distribution of doubly-odd isotopes [30,48,58].

The BW effect may be parametrized as [59]

$$\mathcal{A} = \mathcal{A}_0(1 + \epsilon), \quad (5)$$

where \mathcal{A}_0 is the hyperfine constant with a pointlike magnetization distribution ($F = 1$). Here, \mathcal{A}_0 includes the Breit-Rosenthal (BR) correction δ , due to the finite nuclear charge distribution, which is taken into account by solving the electron wave functions in the field of a finite nucleus (we use a Fermi distribution with rms charge radii from Ref. [60]). This may be expressed as $\mathcal{A}_0 = \mathcal{A}_{00}(1 + \delta)$, where \mathcal{A}_{00} is the hyperfine constant with pointlike nuclear magnetic and charge distributions. Since the nuclear charge distribution is known with relatively high accuracy, errors associated with the BR correction are typically negligible [30,61,62]. Note that radiative quantum electrodynamics (QED) corrections contribute to the hyperfine structure with comparable size to ϵ [28,49,63], though they are largely independent of the isotope and therefore strongly cancel in the differential hyperfine anomaly considered below. Therefore, we do not consider QED contributions further.

We calculate \mathcal{A}_0 using the relativistic Hartree-Fock method, including the important core-polarization contribution by means of the time-dependent Hartree-Fock (TDHF) method [64,65], equivalent to the random phase approximation with exchange (RPA). We consider atoms with a single valence electron above a closed-shell core, for which the valence wave function is found in the Hartree-Fock potential due to the $(N - 1)$ core electrons ($N = Z$ for neutral atoms). The set of TDHF equations,

$$(H - \epsilon_c)\delta\psi_c = -(h_{\text{hfs}} + \delta V - \delta\epsilon_c)\psi_c, \quad (6)$$

is then solved self-consistently for each electron in the core. Here, H , ψ_c , and ϵ_c are the relativistic Hartree-Fock Hamiltonian, core electron orbitals, and core electron binding energies, respectively, and $\delta\psi_c$ and $\delta\epsilon_c$ are hyperfine-induced corrections for core orbitals and energies. The resulting hyperfine-induced correction to the Hartree-Fock potential is given by δV . Since h_{hfs} can mix states with different angular momenta, $\delta\psi_c$ is not an angular momentum eigenstate and contains contributions from states with $j = j_c$, $j_c \pm 1$ (j_c is the angular momentum of single-electron state c). Then, matrix elements for valence states v are calculated as $\langle v|h_{\text{hfs}} + \delta V|v\rangle$, which includes the core-polarization effects to all orders in the Coulomb interaction [65]. Correlation corrections to the hyperfine structure were studied recently by us in detail [66], and those beyond core polarization were shown not to be important for the relative BW effect (see also Refs. [28,29,67,68]). The insensitivity of the relative BW effect to correlations is due to the short-range nature of the effect, with the account of correlations affecting the normalization of the wave functions which largely factors out in the relative correction.

TABLE I. Bohr-Weisskopf corrections ϵ and hyperfine anomalies ${}^1\Delta^2$ calculated in the ball and single-particle (SP) nuclear magnetization models for the lowest states of several atoms of interest, and comparison with experimental differential anomalies. A is the atomic mass number for the isotope, and I^π is the nuclear spin and parity.

		Isotope 1				Isotope 2				Differential anomaly ${}^1\Delta^2$ (%)		
		A	I^π	ϵ_{Ball} (%)	ϵ_{SP} (%)	A	I^π	ϵ_{Ball} (%)	ϵ_{SP} (%)	Ball	SP	Expt. [59]
${}^{37}\text{Rb}$	$5s_{1/2}$	85	$5/2^-$	-0.306	0.044	87	$3/2^-$	-0.306	-0.278	-0.001	0.323	0.35142(30)
						86	2^-	-0.306	-0.139	0.000	0.183	0.17(9)
${}^{47}\text{Ag}$	$5s_{1/2}$	107	$1/2^-$	-0.497	-4.20	103	$7/2^+$	-0.493	-0.347	-0.018	-3.88	-3.4(17)
						109	$1/2^-$	-0.498	-3.78	0.007	-0.431	-0.41274(29)
${}^{55}\text{Cs}$	$6s_{1/2}$	133	$7/2^+$	-0.716	-0.209	131	$5/2^+$	-0.716	-0.596	-0.001	0.389	0.45(5) ^a
						135	$7/2^+$	-0.716	-0.247	0.002	0.039	0.037(9) ^b
						134	4^+	-0.716	-0.371	0.000	0.163	0.169(30)
${}^{56}\text{Ba}^+$	$6s_{1/2}$	135	$3/2^+$	-0.747	-1.03	137	$3/2^+$	-0.747	-1.03	0.001	0.001	-0.191(5)
${}^{70}\text{Yb}^+$	$6s_{1/2}$	171	$1/2^-$	-1.37	-2.41	173	$5/2^-$	-1.38	-1.79	0.014	-0.618	-0.425(5)
${}^{79}\text{Au}$	$6s_{1/2}$	197	$3/2^+$	-1.97	15.5	199	$3/2^+$	-1.97	7.47	0.013	7.48	3.64(29)
${}^{80}\text{Hg}^+$	$6s_{1/2}$	199	$1/2^-$	-2.04	-3.57	201	$3/2^-$	-2.05	-2.20	0.016	-1.39	-0.16257(5)
${}^{81}\text{Tl}$	$7s_{1/2}$	203	$1/2^+$	-2.13	-2.13	205	$1/2^+$	-2.13	-2.13	0.015	0.015	0.0294(81) ^c
${}^{81}\text{Tl}$	$6p_{1/2}$	203	$1/2^+$	-0.780	-0.780	205	$1/2^+$	-0.781	-0.781	0.005	0.005	0.01035(15)

^aReference [69].

^bReference [70].

^cReference [71].

III. DIFFERENTIAL HYPERFINE ANOMALY

The differential hyperfine anomaly ${}^1\Delta^2$ is defined via the ratio of the hyperfine constants for different isotopes of the same atom (see, e.g., Ref. [59]):

$$\frac{\mathcal{A}^{(1)}}{\mathcal{A}^{(2)}} = \frac{g_I^{(1)}}{g_I^{(2)}} (1 + {}^1\Delta^2). \quad (7)$$

This quantity, which is a measure of the deviation of the hyperfine structure from the case of a pointlike nucleus, may be found with high accuracy from experiment, provided the nuclear magnetic moments are known well and determined independently of the hyperfine measurements [59]. As for the theoretical determination of ${}^1\Delta^2$, the correlation corrections beyond RPA that contribute to the hyperfine constants $\mathcal{A}^{(1)}$ and $\mathcal{A}^{(2)}$ cancel in the ratio [66,68], making the electronic structure calculations robust at the level of RPA and of high accuracy. Note that there is a strong cancellation of the BR corrections in the differential anomaly, $\delta^{(1)} - \delta^{(2)}$. For nuclei with different spins, the differential hyperfine anomaly is typically dominated by the BW effect [59],

$${}^1\Delta^2 \approx \epsilon^{(1)} - \epsilon^{(2)}. \quad (8)$$

The comparison of calculated and measured hyperfine anomalies therefore presents a powerful test of the validity of nuclear magnetization models.

In Table I we present our results for the BW effects and differential hyperfine anomalies obtained using the ball (2) and single-particle (3) models. The numerical accuracy for the BW calculations is better than 1%, well below the model uncertainty. We present results for the lowest states of systems of interest for atomic parity violation and electric dipole moment studies, and we also present results for Ag and Au, which may be treated as single-valence-electron systems and for which the BW effects and hyperfine anomalies are particularly

large. The anomaly is calculated using Eq. (7) rather than Eq. (8), which means that the small differential BR effect is included. The calculated values for ${}^1\Delta^2$ are compared against available experimental data [59]. Note that the uncertainties in the measured values are dominated by uncertainties in the nuclear magnetic moments [72].

We draw attention to several points. First, the BW correction is a significant effect, typically entering at the level of several 0.1% to several 1% for the considered systems. For Ag and Au the effect is even larger, contributing at around 10% for Au. Second, the ball and single-particle models often lead to substantially different BW effects. For ${}^{85}\text{Rb}$ and ${}^{133}\text{Cs}$, the difference is as large as 0.4% and 0.5%, respectively, matching or exceeding the atomic structure theory uncertainty [28,30]. Finally, from a comparison of the calculated and measured hyperfine anomalies in Table I, it is seen that the nuclear SP model leads to substantially better agreement with experiment for the majority of cases. The agreement is particularly good for isotopes of Rb, Cs, and Ag, and is reasonably good for Yb^+ . Our results for Au reproduce the (atypical) sign and large size of the effect, and agree well with the SP results of recent atomic many-body calculations [73]. We note that in Ref. [73] it was found that the BW effect for ${}^{197}\text{Au}$ in the SP model is too large to be consistent with a value directly extracted from the measured hyperfine constant, and our own calculations, including correlation corrections, agree with this conclusion. In the ball model, the only difference in the BW effect between isotopes comes from changing the nuclear radius, similarly to the differential BR effect, so the calculated anomaly is always small and the model generally cannot produce the observed anomalies.

Recently, we considered the case of Fr in detail, and we demonstrated using “double” differential hyperfine anomalies [74] that the single-particle model works very well for both odd and doubly-odd isotopes between 207 and 213 [30]

(see also Refs. [54,55,75]). This allowed us to extract nuclear magnetic moments for these isotopes with significantly higher precision than was previously possible. The BW effect is particularly large for these Fr isotopes ($\sim 1\%$ - 2%), and it differs between the ball and SP models by nearly 1.5% for the odd isotopes. This difference is the main reason for the large deviation (up to 2%) of the deduced moments found in Ref. [30] from previous best determinations. In the same work, the validity of the nuclear SP model in the neighborhood of Fr was supported by the BW effect extracted directly from hydrogenlike ^{207}Pb and ^{209}Bi : The calculated and experimental BW results for $^{207}\text{Pb}^{81+}$ are -3.55% and $-3.85(4)\%$, respectively, and for $^{209}\text{Bi}^{82+}$ are -1.07% and $-1.03(5)\%$ (see Ref. [30] and references therein). The nuclear SP results for these H-like systems are in excellent agreement with the results of nuclear many-body calculations [76], which are feasible for simple atomic systems.

It is worth discussing the case of the BW effect in $^{225}\text{Ra}^+$, which was calculated in Ref. [28]. Generally, the size of the atomic structure uncertainties precludes the direct extraction of the BW effect from hyperfine comparisons in many-electron systems. For this system, however, the effect is so large that direct extraction is possible. This was done in Ref. [77] where the value $\epsilon = -4.7\%$ was obtained, which may be compared to the simple SP (and ball) result $\epsilon = -2.8\%$ and to the more sophisticated SP result with the nucleon wave function found in the Woods-Saxon potential and with a spin-orbit interaction included, $\epsilon = -4.3\%$ [28].

The simple nuclear single-particle model does not always work well. This may be seen from Table I for Ba^+ , Hg^+ , and Tl . For the considered isotopes of Hg^+ , the SP model produces a differential hyperfine anomaly that is significantly larger than the observed value. For isotopes of Ba^+ and Tl , the nuclear states are the same, and the SP model produces very similar BW effects which cancel strongly in the anomaly (8). In this case, the neglected nuclear many-body contributions will be more important for the differential anomaly than for the BW effect. Another reason for the discrepancy that appears in the hyperfine anomaly may arise due to the magnetic radius. In our calculations we have taken the magnetic rms radius to be the same as the charge rms radius, though there is no reason for them to be the same. Indeed, there are indications that the magnetic radii for ^{203}Tl and ^{205}Tl are different from one another and from the charge radius [78–80]. It was shown very recently that the nuclear single-particle model outperforms the ball model for several Tl isotopes with different nuclear states [45], and the BW effects extracted from experiments with $^{203,205}\text{Tl}^{80+}$ are in good agreement with nuclear SP calculations [49,78]. For Ba^+ , we can look to the Cs differential anomalies involving ^{134}Cs , with the same neutron configuration as $^{135}\text{Ba}^+$; the coincidence of the SP and experimental results (Table I) lends support to the validity of the model, which describes the magnetization distribution of the unpaired neutron. While the nuclear single-particle model does not always give differential anomalies in good agreement with experiment, it generally performs better than the ball model across the board and is expected to produce more accurate values for the BW effect.

We emphasize that our focus is on testing the validity of a simple nuclear model that may be used readily in atomic

many-body calculations. While differential anomaly data obtained using more sophisticated nuclear models are available (see, e.g., Refs. [81,82]), the corresponding atomic theory treatment is necessarily simplistic. It is worthwhile noting that these data show the complexity and challenge of the nuclear structure problem, and for a number of systems the nuclear single-particle model gives results that are at least as good as those obtained using more sophisticated nuclear models. For example, for the anomaly $^{133}\Delta^{135}$ in Cs, a configuration mixing model gives $0.068(25)\%$ [81], while microscopic nuclear theory gives 0.041% which shifts to 0.057% with the inclusion of $\Delta l = 2$ nuclear core polarization [82].

We finally mention the case of heavy muonic atoms [46,58], for which the BW contribution is so large that it may even exceed the size of the total hyperfine constant (see also recent calculations [83,84], and an experimental program to measure nuclear properties in muonic atoms involving scarce and radioactive elements [85,86]). There are experimental BW data available for a number of muonic atoms [58], and this can inform us further on the validity of the SP model for Hg and Cs. Importantly, this tells us about the BW contribution for a single isotope, which may be readily extracted from measurements. Our SP calculation for muonic ^{199}Hg gives $\epsilon = -85.3\%$, which may be compared to the measured value $-68.7(80)\%$ [58], and is in excellent agreement with more sophisticated calculations [82]. Our result for muonic ^{133}Cs is $\epsilon = -15.5\%$, and the measured value $-18.7(13)\%$ [58], lending strong support for the validity of the single-particle model. These calculations will be presented in more detail elsewhere.

IV. IMPLICATIONS FOR ATOMIC PARITY VIOLATION

We now consider the implications for atomic parity violation studies. The dominant parity-violating effects in atoms arise due to the exchange of neutral weak bosons between atomic electrons and the nucleus, leading to the mixing of atomic states of opposite parity [1]. Such interactions are localized on the nucleus, and the theoretical evaluation of the relevant matrix elements, e.g., $\langle s_{1/2} | \hat{H}_{\text{PV}} | p_{1/2} \rangle$, therefore depends on precise knowledge of the wave functions in this region. These matrix elements cannot be directly compared to experiment, and information about the accuracy of the wave functions and the matrix elements is found from a survey of the deviations between theory and experiment for the hyperfine constants of the relevant states and for the combination $\sqrt{A^s A^p}$, which is considered to give a more reliable indication of the accuracy for the off-diagonal matrix elements [1,8].

Separating out the BW contribution, the relevant quantity becomes

$$\sqrt{A^s A^p} \approx \sqrt{A_0^s A_0^p} [1 + (\epsilon_s + \epsilon_p)/2]. \quad (9)$$

The claimed accuracy of the most precise atomic parity violation calculations for ^{133}Cs are based in part on deviations of the hyperfine constants and the quantity (9) from experiment, where the nuclear magnetization distribution was treated as uniformly distributed (ball model). Correcting the nuclear magnetization model (to single-particle) leads to a significant change in the hyperfine constants for s states by $+0.5\%$. (For

$p_{1/2}$ states, the BW effect is an order of magnitude smaller and the hyperfine constants change by only 0.03%.) Evaluations of the quantity (9) should therefore be shifted by +0.3%, which is large compared to the highest-precision atomic parity violation calculations with claimed uncertainties 0.27%–0.5% [8–12]. The effect of this correction is an increase in the deviation from experiment for the hyperfine $6s$ state and the associated quantity (9) in Ref. [11], while the results of the work [8] are hardly changed when accounting also for QED contributions, which is consistent with the 0.5% claimed uncertainty for the atomic parity violation calculation in that work [8,9]; see the analysis in Ref. [29]. This illustrates the importance of understanding and controlling the nuclear magnetic structure, for both reliable benchmarking and continued development of precision atomic theory, and for assigning atomic theory uncertainty which has ramifications for constraints on new physics.

V. CONCLUSION

Hyperfine comparisons only serve as reliable tests of atomic theory if the nuclear magnetization distribution is

adequately modeled, with uncertainties well below those of atomic theory. This has not been the case for a number of atoms of interest for precision studies, including Cs. In this paper, we point out that sufficient experimental data exist for many isotopes, allowing tests of nuclear magnetization models using hyperfine anomalies. From a study of the hyperfine anomalies, we demonstrate that the single-particle model generally outperforms the near universally used ball model. It is simple enough to include into atomic structure codes without the need for any sophisticated nuclear calculations, and we advocate its use in future studies. These investigations into hyperfine anomalies open a window for probing the nuclear structure, including the neutron distribution.

ACKNOWLEDGMENTS

We thank J. R. Persson for useful comments on the manuscript. This work was supported by the Australian Government through Australian Research Council (ARC) DECRA Fellowship No. DE210101026 and ARC Future Fellowship No. FT170100452.

-
- [1] J. S. M. Ginges and V. V. Flambaum, *Phys. Rep.* **397**, 63 (2004).
 - [2] B. M. Roberts, V. A. Dzuba, and V. V. Flambaum, *Annu. Rev. Nucl. Part. Sci.* **65**, 63 (2015).
 - [3] M. S. Safronova, D. Budker, D. DeMille, D. F. J. Kimball, A. Derevianko, and C. W. Clark, *Rev. Mod. Phys.* **90**, 025008 (2018).
 - [4] P. A. Zyla *et al.* (Particle Data Group), *Prog. Theor. Exp. Phys.* **2020**, 083C01 (2020).
 - [5] C. S. Wood, S. C. Bennett, D. Cho, B. P. Masterson, J. L. Roberts, C. E. Tanner, and C. E. Wieman, *Science* **275**, 1759 (1997).
 - [6] S. C. Bennett and C. E. Wieman, *Phys. Rev. Lett.* **82**, 2484 (1999).
 - [7] G. Toh, A. Damitz, C. E. Tanner, W. R. Johnson, and D. S. Elliott, *Phys. Rev. Lett.* **123**, 073002 (2019).
 - [8] V. A. Dzuba, V. V. Flambaum, and J. S. M. Ginges, *Phys. Rev. D* **66**, 076013 (2002).
 - [9] V. V. Flambaum and J. S. M. Ginges, *Phys. Rev. A* **72**, 052115 (2005).
 - [10] V. M. Shabaev, K. Pachucki, I. I. Tupitsyn, and V. A. Yerokhin, *Phys. Rev. Lett.* **94**, 213002 (2005).
 - [11] S. G. Porsev, K. Beloy, and A. Derevianko, *Phys. Rev. Lett.* **102**, 181601 (2009); *Phys. Rev. D* **82**, 036008 (2010).
 - [12] V. A. Dzuba, J. C. Berengut, V. V. Flambaum, and B. M. Roberts, *Phys. Rev. Lett.* **109**, 203003 (2012).
 - [13] M. Pospelov and A. Ritz, *Ann. Phys. (NY)* **318**, 119 (2005).
 - [14] J. Engel, M. J. Ramsey-Musolf, and U. van Kolck, *Prog. Part. Nucl. Phys.* **71**, 21 (2013).
 - [15] W. B. Cairncross and J. Ye, *Nat. Rev. Phys.* **1**, 510 (2019).
 - [16] T. E. Chupp, P. Fierlinger, M. J. Ramsey-Musolf, and J. T. Singh, *Rev. Mod. Phys.* **91**, 015001 (2019).
 - [17] B. C. Regan, E. D. Commins, C. J. Schmidt, and D. DeMille, *Phys. Rev. Lett.* **88**, 071805 (2002).
 - [18] J. J. Hudson, D. M. Kara, I. J. Smallman, B. E. Sauer, M. R. Tarbutt, and E. A. Hinds, *Nature (London)* **473**, 493 (2011).
 - [19] R. H. Parker, M. R. Dietrich, M. R. Kalita, N. D. Lemke, K. G. Bailey, M. Bishof, J. P. Greene, R. J. Holt, W. Korsch, Z.-T. Lu, P. Mueller, T. P. O'Connor, and J. T. Singh, *Phys. Rev. Lett.* **114**, 233002 (2015).
 - [20] B. Graner, Y. Chen, E. G. Lindahl, and B. R. Heckel, *Phys. Rev. Lett.* **116**, 161601 (2016).
 - [21] W. B. Cairncross, D. N. Gresh, M. C. Grau, K. C. Cossel, T. S. Roussy, Y. Ni, Y. Zhou, J. Ye, and E. A. Cornell, *Phys. Rev. Lett.* **119**, 153001 (2017).
 - [22] P. Aggarwal, H. L. Bethlem, A. Borschevsky, M. Denis, K. Esajas, P. A. B. Haase, Y. Hao, S. Hoekstra, K. Jungmann, T. B. Meijknecht, M. C. Mooij, R. G. E. Timmermans, W. Ubachs, L. Willmann, and A. Zapara, *Eur. Phys. J. D* **72**, 197 (2018).
 - [23] V. Andreev, D. G. Ang, D. DeMille, J. M. Doyle, G. Gabrielse, J. Haefner, N. R. Hutzler, Z. Lasner, C. Meisenhelder, B. R. O'Leary, C. D. Panda, A. D. West, E. P. West, X. Wu, and The ACME Collaboration, *Nature (London)* **562**, 355 (2018).
 - [24] X. Wu, Z. Han, J. Chow, D. G. Ang, C. Meisenhelder, C. D. Panda, E. P. West, G. Gabrielse, J. M. Doyle, and D. DeMille, *New J. Phys.* **22**, 023013 (2020).
 - [25] O. Grasdijk, O. Timgren, J. Kastelic, T. Wright, S. Lamoreaux, D. DeMille, K. Wenz, M. Aitken, T. Zelevinsky, T. Winick, and D. Kowall, *arXiv:2010.01451*.
 - [26] A. Bohr and V. F. Weisskopf, *Phys. Rev.* **77**, 94 (1950).
 - [27] A. Bohr, *Phys. Rev.* **81**, 331 (1951).
 - [28] J. S. M. Ginges, A. V. Volotka, and S. Fritzsche, *Phys. Rev. A* **96**, 062502 (2017).
 - [29] J. S. M. Ginges and A. V. Volotka, *Phys. Rev. A* **98**, 032504 (2018).
 - [30] B. M. Roberts and J. S. M. Ginges, *Phys. Rev. Lett.* **125**, 063002 (2020).
 - [31] S. Aubin, J. A. Behr, R. Collister, V. V. Flambaum, E. Gomez, G. Gwinner, K. P. Jackson, D. Melconian, L. A. Orozco, M. R. Pearson, D. Sheng, G. D. Sprouse, M. Tandecki, J. Zhang, and Y. Zhao, *Hyperfine Interact.* **214**, 163 (2013).

- [32] M. Tandecki, J. Zhang, R. Collister, S. Aubin, J. A. Behr, E. Gomez, G. Gwinner, L. A. Orozco, and M. R. Pearson, *J. Instrum.* **8**, P12006 (2013).
- [33] N. Fortson, *Phys. Rev. Lett.* **70**, 2383 (1993).
- [34] V. A. Dzuba, V. V. Flambaum, and J. S. M. Ginges, *Phys. Rev. A* **63**, 062101 (2001).
- [35] T. W. Koerber, M. Schacht, W. Nagourney, and E. N. Fortson, *J. Phys. B* **36**, 637 (2003).
- [36] R. Pal, D. Jiang, M. S. Safronova, and U. I. Safronova, *Phys. Rev. A* **79**, 062505 (2009).
- [37] P. Mandal, A. Sen, and M. Mukherjee, *Hyperfine Interact.* **196**, 261 (2010).
- [38] O. O. Versolato, L. W. Wansbeek, G. S. Giri, J. E. van den Berg, D. J. van der Hoek, K. Jungmann, W. L. Kruithof, C. J. Onderwater, B. K. Sahoo, B. Santra, P. D. Shidling, R. G. E. Timmermans, L. Willmann, and H. W. Wilschut, *Can. J. Phys.* **89**, 65 (2011).
- [39] V. A. Dzuba, V. V. Flambaum, and B. M. Roberts, *Phys. Rev. A* **86**, 062512 (2012).
- [40] B. M. Roberts, V. A. Dzuba, and V. V. Flambaum, *Phys. Rev. A* **88**, 012510 (2013); **89**, 012502 (2014).
- [41] M. Nuñez Portela, E. A. Dijck, A. Mohanty, H. Bekker, J. E. van den Berg, G. S. Giri, S. Hoekstra, C. J. G. Onderwater, S. Schlessler, R. G. E. Timmermans, O. O. Versolato, L. Willmann, H. W. Wilschut, and K. Jungmann, *Appl. Phys. B* **114**, 173 (2014).
- [42] M. Fan, C. A. Holliman, A. L. Wang, and A. M. Jayich, *Phys. Rev. Lett.* **122**, 223001 (2019).
- [43] D. Antypas, A. Fabricant, J. E. Stalnaker, K. Tsigtukin, V. V. Flambaum, and D. Budker, *Nat. Phys.* **15**, 120 (2019).
- [44] K. Harada, T. Aoki, K. Kato, H. Kawamura, T. Inoue, A. Uchiyama, K. Sakamoto, S. Ito, M. Itoh, T. Hayamizu, A. Hatakeyama, K. Hatanaka, T. Wakasa, and Y. Sakemi, *J. Phys.: Conf. Ser.* **691**, 012017 (2016).
- [45] S. D. Prosnjak and L. V. Skripnikov, *Phys. Rev. C* **103**, 034314 (2021).
- [46] M. Le Bellac, *Nucl. Phys.* **40**, 645 (1963).
- [47] V. M. Shabaev, *J. Phys. B* **27**, 5825 (1994).
- [48] V. M. Shabaev, M. B. Shabaeva, and I. I. Tupitsyn, *Phys. Rev. A* **52**, 3686 (1995).
- [49] V. M. Shabaev, M. Tomaselli, T. Kühn, A. N. Artemyev, and V. A. Yerokhin, *Phys. Rev. A* **56**, 252 (1997).
- [50] I. I. Tupitsyn, A. V. Loginov, and V. M. Shabaev, *Opt. Spectrosc.* **93**, 357 (2002).
- [51] A. V. Volotka, D. A. Glazov, I. I. Tupitsyn, N. S. Oreshkina, G. Plunien, and V. M. Shabaev, *Phys. Rev. A* **78**, 062507 (2008).
- [52] A. E. Barzakh, D. Atanasov, A. N. Andreyev, M. Al Monthery, N. A. Althubiti, B. Andel, S. Antalic, K. Blaum, T. E. Cocolios, J. G. Cubiss, P. Van Duppen, T. D. Goodacre, A. de Roubin, Y. A. Demidov, G. J. Farooq-Smith, D. V. Fedorov, V. N. Fedosseev, D. A. Fink, L. P. Gaffney, L. Ghys *et al.*, *Phys. Rev. C* **101**, 034308 (2020).
- [53] V. Fella, L. V. Skripnikov, W. Nörtershäuser, M. R. Buchner, H. L. Deubner, F. Kraus, A. F. Privalov, V. M. Shabaev, and M. Vogel, *Phys. Rev. Research* **2**, 013368 (2020).
- [54] J. S. Grossman, L. A. Orozco, M. R. Pearson, J. E. Simsarian, G. D. Sprouse, and W. Z. Zhao, *Phys. Rev. Lett.* **83**, 935 (1999).
- [55] J. Zhang, M. Tandecki, R. Collister, S. Aubin, J. A. Behr, E. Gomez, G. Gwinner, L. A. Orozco, M. R. Pearson, and G. D. Sprouse, *Phys. Rev. Lett.* **115**, 042501 (2015).
- [56] V. M. Shabaev, A. N. Artemyev, V. A. Yerokhin, O. M. Zherebtsov, and G. Soff, *Phys. Rev. Lett.* **86**, 3959 (2001).
- [57] L. V. Skripnikov, S. Schmidt, J. Ullmann, C. Geppert, F. Kraus, B. Kresse, W. Nörtershäuser, A. F. Privalov, B. Scheibe, V. M. Shabaev, M. Vogel, and A. V. Volotka, *Phys. Rev. Lett.* **120**, 093001 (2018).
- [58] S. Büttgenbach, *Hyperfine Interact.* **20**, 1 (1984).
- [59] J. R. Persson, *At. Data Nucl. Data Tables* **99**, 62 (2013).
- [60] I. Angeli and K. Marinova, *At. Data Nucl. Data Tables* **99**, 69 (2013).
- [61] H. J. Rosenberg and H. H. Stroke, *Phys. Rev. A* **5**, 1992 (1972).
- [62] T. Heggset and J. R. Persson, *Atoms* **8**, 86 (2020).
- [63] J. Sapirstein and K. T. Cheng, *Phys. Rev. A* **67**, 022512 (2003).
- [64] V. A. Dzuba, V. V. Flambaum, and O. P. Sushkov, *J. Phys. B* **17**, 1953 (1984).
- [65] V. A. Dzuba, V. V. Flambaum, P. G. Silvestrov, and O. P. Sushkov, *J. Phys. B* **20**, 1399 (1987).
- [66] S. J. Grunefeld, B. M. Roberts, and J. S. M. Ginges, *Phys. Rev. A* **100**, 042506 (2019).
- [67] A.-M. Mårtensson-Pendrill, *Phys. Rev. Lett.* **74**, 2184 (1995).
- [68] E. A. Konovalova, Y. A. Demidov, and M. G. Kozlov, *Opt. Spectrosc.* **128**, 1530 (2020).
- [69] R. D. Worley, V. J. Ehlers, W. A. Nierenberg, and H. A. Shugart, *Phys. Rev.* **140**, B1483 (1965).
- [70] H. H. Stroke, V. Jaccarino, D. S. Edmonds, and R. Weiss, *Phys. Rev.* **105**, 590 (1957).
- [71] T.-L. Chen, I. Fan, H.-C. Chen, C.-Y. Lin, S.-E. Chen, J.-T. Shy, and Y.-W. Liu, *Phys. Rev. A* **86**, 052524 (2012).
- [72] N. J. Stone, *At. Data Nucl. Data Tables* **90**, 75 (2005).
- [73] Y. A. Demidov, E. A. Konovalova, R. T. Imanbaeva, M. G. Kozlov, and A. E. Barzakh, *Phys. Rev. A* **103**, 032824 (2021).
- [74] J. R. Persson, *Eur. Phys. J. A* **2**, 3 (1998).
- [75] E. A. Konovalova, Y. Demidov, M. G. Kozlov, and A. Barzakh, *Atoms* **6**, 39 (2018).
- [76] R. A. Sen'kov and V. F. Dmitriev, *Nucl. Phys. A* **706**, 351 (2002).
- [77] L. V. Skripnikov, *J. Chem. Phys.* **153**, 114114 (2020).
- [78] P. Beiersdorfer, S. B. Utter, K. L. Wong, J. R. Crespo López-Urrutia, J. A. Britten, H. Chen, C. L. Harris, R. S. Thoe, D. B. Thorn, E. Träbert, M. G. H. Gustavsson, C. Forsén, and A.-M. Mårtensson-Pendrill, *Phys. Rev. A* **64**, 032506 (2001).
- [79] S. D. Prosnjak, D. E. Maison, and L. V. Skripnikov, *J. Chem. Phys.* **152**, 044301 (2020).
- [80] B. M. Roberts, P. G. Ranclaud, and J. S. M. Ginges (to be published).
- [81] H. H. Stroke, R. J. Blin-Stoyle, and V. Jaccarino, *Phys. Rev.* **123**, 1326 (1961).
- [82] T. Fujita and A. Arima, *Nucl. Phys. A* **254**, 513 (1975).
- [83] A. A. Elizarov, V. M. Shabaev, N. S. Oreshkina, and I. I. Tupitsyn, *Nucl. Instrum. Methods Phys. Res. Sect. B* **235**, 65 (2005).
- [84] N. Michel, N. S. Oreshkina, and C. H. Keitel, *Phys. Rev. A* **96**, 032510 (2017).
- [85] A. Antognini, N. Berger, T. E. Cocolios, R. Dressler, R. Eichler, A. Eggenberger, P. Indelicato, K. Jungmann, C. H. Keitel, K. Kirch, A. Knecht, N. Michel, J. Nuber, N. S. Oreshkina, A. Ouf, A. Papa, R. Pohl, M. Pospelov, E. Rapisarda, N. Ritjoho *et al.*, *Phys. Rev. C* **101**, 054313 (2020).
- [86] A. Knecht, A. Skawran, and S. M. Vogiatzi, *Eur. Phys. J. Plus* **135**, 777 (2020).